

Many-body effects in the one-dimensional electron gas with short-range interaction

A. Gold

Laboratoire de Physique des Solides, Université Paul Sabatier, 118 Route de Narbonne, F-31062 Toulouse, France

(Received 3 February 1995; revised manuscript received 11 October 1996)

We discuss interaction effects for the one-dimensional electron gas with a repulsive δ -function interaction potential by using the random-phase approximation *and* a local-field correction. Analytical results for the local-field correction of charge-density fluctuations and spin-density fluctuations are obtained. The ground-state energy is found to be in better agreement with the exact result than the ground-state energy calculated within the random-phase approximation. We calculate the pair-correlation functions for electrons with parallel and antiparallel spins and the paramagnetic susceptibility. The energies of the collective density modes $\omega_d(q)$ and the collective spin modes $\omega_s(q)$ are calculated and compared with the energy of the electron-hole excitations $\omega_{eh\pm}(q)$: $\omega_d(q \rightarrow 0) > \omega_{eh\pm}(q \rightarrow 0) > \omega_s(q \rightarrow 0)$. The critical exponents for the long-distance behavior of correlation functions are found to be described by local-field corrections. We compare our results for the critical exponents with recent results obtained by bosonization techniques and the conformal field theory. [S0163-1829(97)04415-9]

I. INTRODUCTION

In connection with the long-range Coulomb interaction potential for the interacting electron gas the random-phase approximation (RPA), a mean-field theory describes the ground-state energy and the excitation spectrum in the limit of weak coupling, e.g., for a small RPA parameter r_s (high electron density).¹ Deviations from the RPA can be described within the concept of the local-field correction (LFC).² This concept was successfully used in a self-consistent calculation for electron gases by Singwi, Tosi, Land, and Sjölander (STLS).³

The ground-state energy of a one-dimensional electron gas with a repulsive δ -function interaction potential⁴ can be calculated exactly.⁵ In the following we use the RPA as the mean-field theory. The RPA becomes wrong for a large interaction potential. We will show that the RPA can be improved by the so-called LFC representing many-body effects beyond the mean-field theory.

In two recent papers we considered many-body effects for a Bose condensate⁶ and an electron gas⁷ with long-range Coulomb interaction by using an analytical form of the static-structure factor (SSF). It was shown that with increasing valley degeneracy the correlation energy increases.⁸ The one-dimensional Bose condensate with short-range interaction, where exchange effects are not present, is a model system, where analytical results for the LFC and the pair-correlation function can be obtained.⁹ Exchange effects have to be taken into account for a one-dimensional electron gas with short-range interaction. In this paper we show that, using an analytical form of the SSF,^{6,7,9} one obtains transparent analytical results for the LFC and the ground-state energy. By comparing our results with exact results and numerical results within the STLS approach,⁵ we show that the analytical form of the SSF is indeed a very good approximation.

The effect of a finite valley degeneracy in the case of a short-range interaction is studied. In quantum wire structures made from GaAs/Al_xGa_{1-x}As, the valley degeneracy $g_v = 1$. However, it was shown in experiment that the valley degeneracy

in wire structures based on Si_xGe_{1-x} is $g_v = 2$.¹⁰ This motivates our study of the valley degeneracy. The study of the limit $g_v \rightarrow \infty$ is motivated by recent experimental results concerning the collective modes of a Bose condensate,¹¹ and theoretical work concerning the possibility of a Bose condensation in one dimension.¹²

Spin fluctuations can be treated by introducing the LFC for the spin susceptibility, and result in a Stoner-like enhancement factor. The Lobo, Singwi, and Tosi (LST) approach¹³ uses the concept of the LFC for the spin susceptibility for the electron gas with long-range Coulomb interaction. We use our analytical approach for density fluctuations in order to treat spin fluctuations for a short-range interaction potential.

In recent years intense activity in condensed-matter theory was directed toward the Luttinger liquid and the Hubbard model in one dimension, in order to understand better correlation effects. For a review, see Ref. 14. Both models can be solved exactly.¹⁵ More recent methods to calculate many-body effects are bosonization techniques¹⁶ and the conformal field theory.¹⁷ For the Hubbard model, critical exponents for the long-distance behavior of correlation functions have been calculated. Using the analytical results obtained in this paper, it is pointed out that the theory of STLS and LST allows us to make contact with recently developed approaches. By studying the pair-correlation function $g(z \rightarrow \infty)$, we derive critical exponents for our model, and we compare and discuss similarities and differences with diagrammatic (weak-coupling) results,¹⁸ exact results,¹⁵ results obtained by bosonization techniques,¹⁶ and the conformal field theory.¹⁷ Doing this we supply arguments about how to relate the "older" many-body theory (using the concept of the LFC) with more "recent" work in this field (using bosonization techniques and conformal field theory).

The paper is organized as follows. In Sec. II we describe the model. Our theory and the results for charge fluctuations are derived and discussed in Sec. III. In Sec. IV we present the theory and the results for spin fluctuations. We discuss our theory in connection with other theoretical work in Sec.

V. We explain the relevance of the local-field correction in connection with critical exponents in Sec. VI. We comment on some experimental work in Sec. VII. The conclusion is presented in Sec. VIII.

II. MODEL

We study a one-dimensional electron model with kinetic energy, characterized by an effective mass m , and interaction energy characterized by the potential V_0 . The interaction potential between two particles at r_1 and r_2 is given by $V(r_1, r_2) = V_0 \delta(r_1 - r_2)$. In the Fourier space the interaction potential is independent of the wave number q and expressed as $V(q) = V_0$. The electron density n and the electron mass define, together with V_0 , the relevant dimensionless parameter γ for the strength of the interaction as

$$\gamma = mV_0/n = \pi C_p/2g_v. \quad (1)$$

The parameter C_p was introduced before.^{5,19} g_v is the valley degeneracy. The electron density defines the Fermi wave number k_F via $n = 2g_v k_F/\pi$. We express all results as functions of γ . The parameter γ depends on n and V_0 , and γ is small for large density and (or) small V_0 . Our results, which we derive in the following, depend on γ and g_v or C_p and g_v . $V_0 = h^2 b/\pi m$ characterizes the interaction of electrons with scattering length b . h is Planck's constant. In the following, we use $h = 2\pi$.

III. CHARGE FLUCTUATIONS

A. Theory

For a short-range interaction potential the LFC is independent of the wave number,⁵ and the dynamic density response function $\mathbf{X}(q, \omega)$ is given by

$$\mathbf{X}(q, \omega) = \frac{\mathbf{X}_0(q, \omega)}{1 + V_0[1 - G(\gamma)]\mathbf{X}_0(q, \omega)}. \quad (2)$$

$\mathbf{X}_0(q, \omega)$ is the Lindhard function of the one-dimensional free electron gas. $G(\gamma)$ is the LFC for density fluctuations, and was discussed before.^{5,19} Collective modes are defined by poles of the response functions: $1/\mathbf{X}(q, \omega_d(q)) = 0$ describes the collective modes $\omega_d(q)$ for density (d) excitations (zero sound).

Within the STLS approach, the LFC is given by⁵

$$G_{\text{STLS}} = \frac{1}{\pi n} \int_0^\infty dq [1 - S(q)]. \quad (3)$$

In the following we use $G(\gamma) = G_{\text{STLS}}$. $S(q)$ is the SSF and, following the arguments given in Refs. 6, 7, and 9, we use the analytical expression

$$S(q) = \frac{1}{[1/S_0(q)^2 + 4n^2\gamma[1 - G(\gamma)]/q^2]^{1/2}}. \quad (4)$$

$S_0(q)$ is the SSF of the noninteracting electron gas. The factor containing $\gamma[1 - G(\gamma)]$ represents the contribution of the collective modes to the SSF. Equation (4) takes into account one-particle excitations and sound modes with $S(q \rightarrow 0) \propto q$. The SSF in Eq. (4) corresponds to a *generalized* Feynman-Bijl form, where one-particle excitations and

collective excitations are taken into account. If one-particle excitations are not present, as for a Bose condensate where $S_0(q) = 1$, one obtains the Feynman-Bijl form.² The detailed form of the SSF reflects the structure $1/\mathbf{X}_0(q, \omega) + V_0[1 - G(\gamma)]$ in $\mathbf{X}(q, \omega)$. Equations (3) and (4) can be solved analytically by using $S_0(q \leq 2k_F) = q/2k_F$ and $S_0(q > 2k_F) = 1$ for the one-dimensional free-electron gas.

With $S_0(q) = 1$ we obtain the SSF of the Bose gas, where the expression is exact. This model was studied before, and analytical results for the LFC have been obtained.⁹ For an electron gas, exchange effects have to be taken into account via $S_0(q)$. Equation (4) for an electron gas represents an approximation, and this approximation allows us to derive analytical results for the LFC. The validity range can only be judged after comparison with results where this approximation has not been performed as in Ref. 5. It should be noted that this approximation was also used in Ref. 7 for an electron gas with long-range Coulomb interaction, where exact results are not available. It is one of the issues of this paper to show that the analytical expression for the SSF is a good approximation.

With Eqs. (3) and (4), we find

$$G(\gamma) = \frac{1}{2g_v} \frac{1 + 8g_v^2\gamma[1 - G(\gamma)]/\pi^2}{[1 + 4g_v^2\gamma[1 - G(\gamma)]/\pi^2]^{1/2}}. \quad (5)$$

Equation (5) represents a cubic equation for $G(\gamma)$. An explicit solution of the cubic equation will not be given in this paper. However, it is not difficult to obtain numerical results for the relevant solution of the cubic equation with $1/2g_v \leq G(\gamma) \leq 1$. For a large valley degeneracy $g_v \rightarrow \infty$, only the terms in Eq. (5) containing g_v survive, and we find $G(\gamma) = 2[\gamma[1 - G(\gamma)]]^{1/2}/\pi$, which is the result for a Bose condensate in one dimension.⁹ This equation corresponds to a quadratic equation for the LFC. For $g_v \rightarrow \infty$ the kinetic and exchange energies vanish, and the only energy which stays finite, the limit $g_v \rightarrow \infty$, is the correlation energy. This limit was discussed in detail for a long-range interaction potential in Ref. 8.

The lowest-order result is obtained by setting $G(\gamma) = 0$ on the right-hand side of Eq. (5). This is the RPA for the LFC. We find

$$G_{\text{RPA}}(\gamma) = \frac{1}{2g_v} \frac{1 + 8g_v^2\gamma/\pi^2}{[1 + 4g_v^2\gamma/\pi^2]^{1/2}}. \quad (6)$$

The first term in Eq. (6) with $G_{\text{RPA}}(\gamma=0) = G_{\text{HFA}} = 1/2g_v$ represents the exchange term or the Hartree-Fock approximation (HFA) of the LFC. The asymptotic law for weak coupling is written as

$$G(\gamma \rightarrow 0) = \frac{1}{2g_v} \left[1 + (1 - 1/2g_v) \frac{6g_v^2}{\pi^2} \gamma + O(\gamma^2) \right]. \quad (7)$$

The term linear in γ represents correlation effects. The expressions given in Eqs. (6) and (7) strongly overestimate correlation effects. For strong coupling ($\gamma \rightarrow \infty$), we find

$$G(\gamma \rightarrow \infty) = 1 - \pi^2 \delta/8\gamma, \quad (8)$$

With $\delta = 1 - 1/g_v^2 + (1 + 2/g_v^2)^{1/2}$. For $g_v = 1$ we obtain $\delta = 1.73$, and for $g_v = \infty$ we obtain the result of the Bose condensate, where $\delta = 2$.⁹ $G(\gamma)$ versus γ according to Eq.

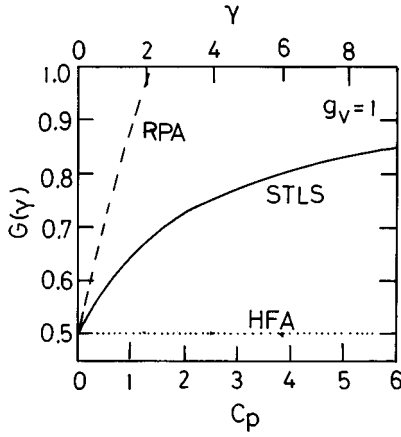


FIG. 1. Local-field correction $G(\gamma)$ vs interaction strength γ (or C_p) according to Eq. (5). The asymptotic results (the RPA and HFA for the LFC) are shown as dotted and dashed lines, respectively.

(5), and the LFC within the RPA and HFA are shown in Fig. 1. Note the small regime of validity of the LFC in the RPA and HFA. In general we find $G_{\text{HFA}} < G(\gamma) < G_{\text{RPA}}(\gamma)$.

B. Pair-correlation function

The pair-correlation function $g(z)$, the probability for finding two electrons at distance z , is given by the SSF,¹ and is expressed as

$$g(\gamma, z) = 1 - \frac{1}{\pi n} \int_0^\infty dq \cos(qz) [1 - S(q)]. \quad (9)$$

For $z=0$, one obtains³ $g(\gamma, z=0) = 1 - G(\gamma)$. For $\gamma \rightarrow 0$ we find $g(\gamma, z=0) = 1 - 1/2g_v - (3g_v - 3/2)\gamma/\pi^2$, and for $g_v=1$ a negative pair correlation is found for $\gamma > \pi^2/3 = 3.3$. This shows that the weak-coupling result for the LFC overestimates correlation effects. For $\gamma \rightarrow \infty$ we derive $g(\gamma, z=0) = \pi^2 \delta/8\gamma$. In charged Coulomb systems, for a large RPA parameter (strong coupling), one finds the unphysical result $g(0) < 0$.³ For an electron gas with contact interaction we find $g(0) > 0$ for an arbitrary strength of the interaction.

$g(\gamma, z=0)$ versus γ is shown in Fig. 2 for $g_v=1$ as the dashed line. Numerical results for this model within the ladder approximation¹⁹ are shown by the solid line. The ground-state energy calculated within the ladder approximation is very near to the exact result. It becomes evident from Fig. 2 that the LFC within the STLS approach is not exact; however, it describes the main effects due to interactions. Most important is the fact that the results of the STLS approach, using the analytical form of the SSF and shown as the dashed line in Fig. 2, are nearly identical to the results using a numerically determined SSF,^{5,9} shown as solid dots in Fig. 2.

C. Ground-state energy

The interaction energy $\epsilon_{\text{int}}(\gamma)$ is given in terms of the SSF. Within the STLS approach one finds $\epsilon_{\text{int}}(\gamma) = n^2 \gamma [1 - G(\gamma)]/2m$. We note that the term linear in γ represents the Hartree term. The second part represents the interaction en-

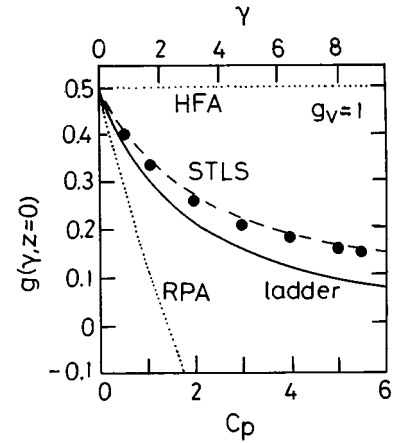


FIG. 2. Pair-correlation function $g(\gamma, z=0)$ vs interaction strength γ (or C_p) as the dashed line. The solid line represents the ladder approximation (Ref. 19). The solid dots are numerical results within the STLS approach (Refs. 5 and 19). The dotted lines represent the RPA and the HFA.

ergy due to exchange and correlation effects. We conclude that $\epsilon_{\text{int}}(\gamma) \propto \gamma g(\gamma, z=0)$. For $\gamma \rightarrow \infty$, we find $\epsilon_{\text{int}}(\gamma)/(n^2/2m) = \pi^2 \delta/8$.

The contribution of the interaction energy to the ground-state energy per particle is expressed as

$$\epsilon_{\text{int}} = \int_0^\gamma d\lambda \frac{\epsilon_{\text{int}}(\lambda)}{\lambda}. \quad (10)$$

The contribution of the kinetic energy to the ground-state energy per particle is given by $\epsilon_F/3 = (\pi^2/12g_v^2)n^2/2m$, and the ground-state energy ϵ_0 is written as

$$\epsilon_0 = \frac{n^2}{2m} \left[\frac{\pi^2}{12g_v^2} + \int_0^\gamma d\lambda [1 - G(\lambda)] \right], \quad (11)$$

and the total energy is $\epsilon_{\text{tot}} = n\epsilon_0$. Within the RPA for the LFC [see Eq. (6)], the total energy is given by

$$\begin{aligned} \frac{\epsilon_{\text{tot}}}{\epsilon_F k_F} &= \frac{2g_v}{3\pi} + \frac{8g_v^3}{\pi^3} \gamma - \frac{2}{3\pi} \left[1 - \left[1 - \frac{8g_v^2}{\pi^2} \gamma \right] \right. \\ &\quad \left. \times \left[1 + \frac{4g_v^2}{\pi^2} \gamma \right]^{1/2} \right]. \end{aligned} \quad (12)$$

With Eq. (12), for $\gamma \ll 1$ we derive the weak-coupling result as

$$\begin{aligned} \epsilon_0 &= \frac{n^2}{2m} \left[\frac{\pi^2}{12g_v^2} + \gamma - \frac{\gamma}{2g_v} - \frac{18g_v}{24\pi^2} \gamma^2 + \frac{5g_v^3}{3\pi^4} \gamma^3 \right. \\ &\quad \left. + O(g_v^{2k-3} \gamma^k) \right], \end{aligned} \quad (13)$$

with $k > 3$. We mention that the Hartree energy ϵ_H can be written as $\epsilon_H = nV_0/2 = n^2 \gamma/2m$. The first, second, and third terms in Eq. (13) represent the kinetic, Hartree, and exchange energy, respectively. The terms with $-\gamma^2$ and $+\gamma^3$ represent the first corrections due to correlation effects.

The exact strong coupling result for $\gamma \rightarrow \infty$ was calculated in Ref. 20 as $\epsilon_0 = n^2(\pi^2/3)/2m$, which is the ground-state

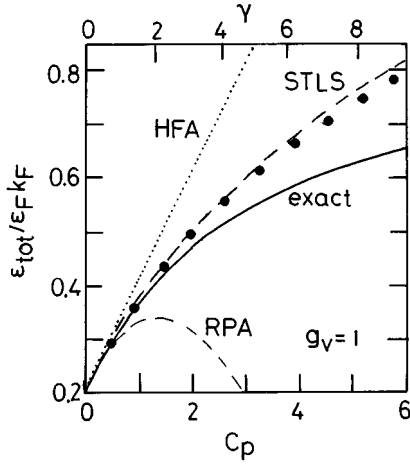


FIG. 3. Total energy ϵ_{tot} (normalized to $\epsilon_F k_F$) vs interaction strength γ (or C_p) according to Eq. (11) as the dashed line. The solid line is the exact result according to Ref. 5. The solid dots are numerical results within the STLS approach (Ref. 5). The HFA and RPA for the LFC are shown as the dotted and dashed lines, respectively.

energy of a Bose condensate.²¹ With $g(\gamma \rightarrow \infty, z=0) \propto 1/\gamma$ it becomes clear that the ground-state energy as calculated within the STLS approach, diverges for large coupling: $\epsilon_0 \propto \ln \gamma$ and we conclude that the STLS approach is not in agreement with the exact result. A similar conclusion was derived for the Bose condensate in one dimension.⁹

The total energy ϵ_{tot} versus γ is shown in Fig. 3 in different approximations. Exact results according to Ref. 5 are shown as the solid line. From Fig. 3 it becomes clear that the RPA and HFA have only a very small validity range: $\gamma < 1$. The finite LFC within the STLS approach strongly increases the validity range of the theory: $\gamma < 10$. The comparison between the numerical result of the STLS approach⁵ and our result, using an analytical form of the SSF, shows that our analytical expression for the SSF is a very powerful approximation.

D. Density susceptibility

With $\mathbf{X}_0(q) = \mathbf{X}_0(q, \omega=0)$, the static density susceptibility $\mathbf{X}(q) = \mathbf{X}(q, \omega=0)$ is given by

$$\mathbf{X}(q) = \frac{\mathbf{X}_0(q)}{1 + V_0[1 - G(\gamma)]\mathbf{X}_0(q)}. \quad (14)$$

ρ_F is the density of states of the free-electron gas with $\mathbf{X}_0(q \rightarrow 0) = \rho_F = n/2\epsilon_F$ and one finds $V_0\mathbf{X}_0(q \rightarrow 0) = 4g_v^2\gamma/\pi^2$. For the density susceptibility in the long-wavelength limit, we obtain

$$\mathbf{X}(q \rightarrow 0)/\rho_F = \frac{1}{1 + 4g_v^2\gamma[1 - G(\gamma)]/\pi^2}. \quad (15)$$

For small coupling, we find $\mathbf{X}(q \rightarrow 0)/\rho_F = 1 - 4g_v^2\gamma(1 - 1/2g_v)/\pi^2$. For large coupling, we obtain $\mathbf{X}(q \rightarrow 0)/\rho_F = 1/[1 + g_v^2\delta/2]$.

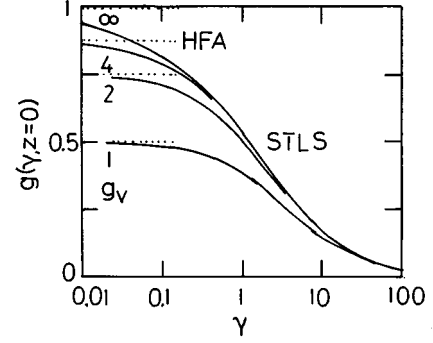


FIG. 4. Pair-correlation function $g(\gamma, z=0)$ vs interaction strength γ for different valley degeneracies. The HFA is shown as the dotted line. The valley degeneracy $1/g_v=0$ corresponds to the Bose condensate (Ref. 9).

E. Valley degeneracy

The valley degeneracy is a very important parameter in semiconductors.²² For instance, the conduction band of silicon shows a valley degeneracy of 6. Wire systems made with a $\text{Si}_x\text{Ge}_{1-x}/\text{Si}$ heterostructure are characterized by a twofold valley degeneracy.¹⁰ For the long-range Coulomb interaction we have shown recently that exchange effects decrease with increasing valley degeneracy while correlation effects increase with increasing valley degeneracy.⁸ This effect is also present for a short-range potential. From the ground-state energy calculated in the RPA, we conclude that the kinetic and exchange energies decrease with increasing valley degeneracy, while the (absolute value of) correlation terms increase with increasing valley degeneracy. Note that the Hartree energy is independent of the valley degeneracy. We mention that our equations for the LFC, the pair-correlation function, and the ground-state energy approach the corresponding values for a Bose condensate if g_v becomes large.

In Fig. 4 we show the pair-correlation function versus γ for different valley degeneracies. Due to the decrease of the exchange term the pair-correlation function increases with increasing valley degeneracy if $\gamma < 2$. For large γ the pair-correlation function is determined by correlation effects. In this case $g(\gamma, z=0)$ is given by δ , and for large valley degeneracy δ approaches the value $\delta=2$ for a Bose condensate.

The ground-state energy ϵ_0 versus coupling parameter γ is shown in Fig. 5 for different valley degeneracies. For large valley degeneracy we obtain the ground-state energy of the Bose condensate.⁹ For small coupling the ground-state energy decreases strongly with increasing valley degeneracy due to the decrease of the kinetic and exchange energies. Note that for large coupling the ground-state energy varies weakly with the valley degeneracy due to the fact that the ground-state energy is determined by the correlation energy, which is determined by δ and δ depends only weakly on g_v .

In Ref. 22 the valley-occupancy phase transition was discussed: for small (large) r_s the ground-state energy of a two-dimensional electron gas with $g_v=2$ is smaller (larger) than for $g_v=1$. This behavior should lead to a valley-occupancy phase transition at a critical RPA parameter. From our results shown in Fig. 5, we conclude that such a phase transition is not expected to occur in one-dimensional systems with a short-range interaction potential. We find that

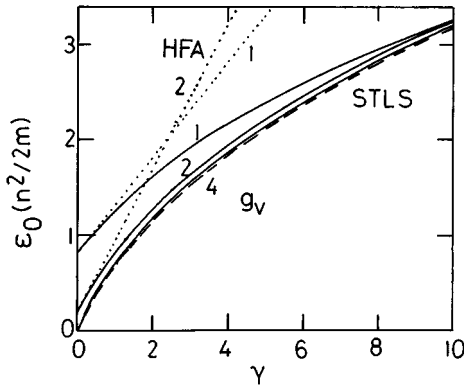


FIG. 5. Ground-state energy ϵ_0 vs interaction strength γ . The solid lines represent the results according to the STLS for valley degeneracy $g_v=1, 2$, and 4 . The dashed line corresponds to our calculation for a Bose condensate ($g_v=\infty$) (Ref. 9). The dotted lines represent the result in the HFA for $g_v=1$ and 2 .

$\epsilon_0(g_v=1) > \epsilon_0(g_v=2) > \epsilon_0(g_v=4)$, and a crossing of the ground-state energy for different valley degeneracy is absent. However, we observe in Fig. 5 that such a valley-occupancy phase transition is expected if the ground-state energy is calculated within the HFA. We conclude that the HFA cannot be used to obtain information about the existence of this phase transition. For a long-range Coulomb interaction such a valley-occupancy phase transition could exist, as discussed recently.²³

IV. SPIN FLUCTUATIONS

A. Theory

The dynamic spin response function $\mathbf{X}_s(q, \omega)$ is written as

$$\mathbf{X}_s(q, \omega) = \frac{\mathbf{X}_0(q, \omega)}{1 - V_0 G_s(\gamma) \mathbf{X}_0(q, \omega)}. \quad (16)$$

$G_s(\gamma)$ is the LFC for spin fluctuations. $\mathbf{X}_M(q, \omega) = g_0^2 \mu_B^2 \mathbf{X}_s(q, \omega)$ is the generalized magnetic susceptibility, and $g_0 \mu_B$ is the magnetic moment of an electron. $1/\mathbf{X}_s(q, \omega_s(q)) = 0$ defines the collective modes $\omega_s(q)$ for spin (s) excitations.

We apply the LST approach,¹³ and the LFC is given by

$$G_{\text{LST}} = \frac{1}{\pi n} \int_0^\infty dq [1 - S_s(q)]. \quad (17)$$

In the following we use $G_s(\gamma) = G_{\text{LST}}$. $S_s(q)$ is the SSF for spin fluctuations, and we use the analytical expression

$$S_s(q) = \frac{1}{[1/S_0(q)^2 - 4n^2 \gamma G_s(\gamma)/q^2]^{1/2}}. \quad (18)$$

Note the minus sign in Eq. (18), which represents the minus sign in Eq. (16). For small wave numbers one finds $S_s(q \rightarrow 0) \propto q$. We mention that $S_s(q)$ is given by the frequency integral over $\mathbf{X}_s(q, \omega)$, which cannot be calculated analytically. We shall show that the pair-correlation function for parallel spins $g_{\uparrow\uparrow}(\gamma, z=0)$, given by $G_s(\gamma)$ and $G(\gamma)$, is very small, which implies that our analytical results for $G_s(\gamma)$, by using $S_s(q)$, fulfill the condition $g_{\uparrow\uparrow}(\gamma, z=0) = 0$ in a very good approximation.

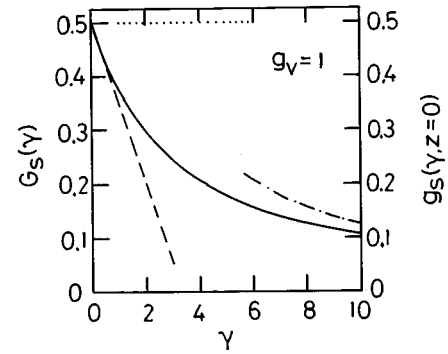


FIG. 6. Local-field correction $G_s(\gamma)$ vs interaction strength γ according to Eq. (19). The asymptotic results according to Eqs. (21) and (22) are shown as dashed and dash-dotted lines, respectively.

Equation (17) can be solved analytically, and we find

$$G_s(\gamma) = \frac{1}{2g_v} \frac{1 - 8g_v^2 \gamma G_s(\gamma)/\pi^2}{[1 - 4g_v^2 \gamma G_s(\gamma)/\pi^2]^{1/2}}. \quad (19)$$

Equation (19) represents a cubic equation for $G_s(\gamma)$. We obtain numerical results for the relevant solution of the cubic equation with $0 \leq G_s(\gamma) \leq 1/2g_v$. From Eq. (19), it becomes clear that the parameter for weak coupling is $g_v \gamma \ll 1$ (and not γ), and the valley degeneracy is an important parameter of the system: we note that $G_s(\gamma=0) = 1/2g_v = G_{s, \text{HFA}}$, and g_v is an independent parameter besides γ .

The first-order approximation (FOA) for the LFC is obtained by using the zero-order result $G_{s, \text{HFA}} = 1/2g_v$ on the right-hand side of Eq. (19), and we obtain

$$G_{s, \text{FOA}}(\gamma) = \frac{1}{2g_v} \frac{1 - 4g_v \gamma/\pi^2}{[1 - 2g_v \gamma/\pi^2]^{1/2}}. \quad (20)$$

The asymptotic law for weak coupling is written as

$$G_s(\gamma \rightarrow 0) = \frac{1}{2g_v} \left[1 - \frac{3g_v}{\pi^2} \gamma + O(\gamma^2) \right]. \quad (21)$$

The term linear in γ represents correlation effects. However, the expressions given in Eqs. (20) and (21) strongly overestimate correlation effects. For strong coupling we find

$$G_s(\gamma \rightarrow \infty) = \pi^2/8g_v^2 \gamma. \quad (22)$$

From this behavior it becomes clear that $G_s(\gamma) = 0$ for $g_v \rightarrow \infty$. For $g_v = 1$ we show $G_s(\gamma)$ versus γ according to Eq. (19) in Fig. 6 together with the asymptotic results according to Eqs. (21) and (22): the asymptotic laws have a small range of validity.

B. Pair-correlation function

The pair-correlation function $g_s(\gamma, z)$, the probability for finding two electrons at distance z , is given by the SSF, and is expressed as

$$g_s(\gamma, z) = \frac{1}{\pi n} \int_0^\infty dq \cos(qz) [1 - S_s(q)]. \quad (23)$$

With Eq. (17) one obtains $g_s(\gamma, z=0) = G_s(\gamma)$. For $\gamma \rightarrow 0$, with Eq. (21), we derive $g_s(\gamma, z=0) = [1 - 3g_v \gamma/\pi^2$

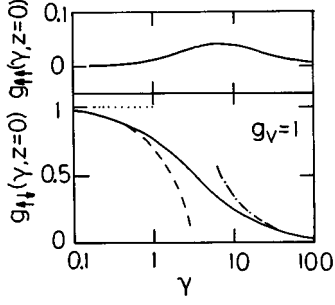


FIG. 7. Pair-correlation function $g_{\uparrow\uparrow}(\gamma, z=0)$ and $g_{\uparrow\downarrow}(\gamma, z=0)$ vs interaction strength γ according to Eq. (24). The asymptotic results for $g_{\uparrow\downarrow}(\gamma, z=0)$ according to Eqs. (25b) and (26b), respectively, are shown as dashed and dash-dotted lines, respectively.

+ $O(\gamma^2)$]/ $2g_v$, and a negative value for $g_s(\gamma, z=0)$ is found for $\gamma > \pi^2/3g_v$, which shows that the weak-coupling result for the LFC strongly overestimates correlation effects. For $\gamma \rightarrow \infty$, we obtain $g_s(\gamma, z=0) = \pi^2/8g_v^2\gamma$.

$G(\gamma)$ and $G_s(\gamma)$ define the pair-correlation functions $g(\gamma, z)$ and $g_s(\gamma, z)$, respectively. We note that

$$g_{\uparrow\uparrow}(\gamma, z) = g(\gamma, z) - g_s(\gamma, z) \quad (24a)$$

and

$$g_{\uparrow\downarrow}(\gamma, z) = g(\gamma, z) + g_s(\gamma, z). \quad (24b)$$

$g_{\uparrow\uparrow}(\gamma, z)$ is the pair-correlation function for parallel spins, and the Pauli principle implies $g_{\uparrow\uparrow}(\gamma, z=0) = 1 - G(\gamma) - G_s(\gamma) \equiv 0$: this behavior reflects the exchange hole in $g_{\uparrow\uparrow}(\gamma, z)$. $g_{\uparrow\downarrow}(\gamma, z)$ is the pair-correlation function for antiparallel spins and for weak coupling, the HFA implies $g_{\uparrow\downarrow}(\gamma \rightarrow 0, z=0) = 1 - G(\gamma) + G_s(\gamma) = 1$, while for strong coupling the repulsion effects lead to $g_{\uparrow\downarrow}(\gamma \rightarrow \infty, z=0) = 0$: this behavior reflects the ‘‘Coulomb’’ hole (the interaction hole) in $g_{\uparrow\downarrow}(\gamma \rightarrow \infty, z)$.

Numerical results for $g_{\uparrow\uparrow}(\gamma, z=0)$ and $g_{\uparrow\downarrow}(\gamma, z=0)$ versus γ are shown in Fig. 7 for $g_v = 1$. $g_{\uparrow\uparrow}(\gamma, z=0) < 0.04$ is slightly positive, which is an artifact of the approach used. $g_{\uparrow\downarrow}(\gamma, z=0)$ decreases with increasing coupling: see Fig. 7. In charged Coulomb systems in three dimensions and for a RPA parameter r_s between $1 < r_s < 6$ the (unphysical) result $g_{\uparrow\uparrow}(0) \approx -0.07$ was reported.¹³ For an electron gas in one dimension with contact interaction, we find $0 < g_{\uparrow\uparrow}(\gamma, z=0) < 0.04$ for an arbitrary strength of the interaction. We believe that this small value for $g_{\uparrow\uparrow}(\gamma, z=0)$ is an important indication that the STLS and LST approach work reasonably well for short-range potentials.

From our analytical results for $g(\gamma, z=0)$ and $g_s(\gamma, z=0)$, for weak coupling we derive

$$g_{\uparrow\uparrow}(\gamma \rightarrow 0, z=0) = 1 - \frac{1}{g_v} + \frac{3}{\pi^2} [1 - g_v] \gamma + \frac{g_v}{2\pi^4} [10g_v^2 + 8g_v - 13] \gamma^2 + O(\gamma^3) \quad (25a)$$

and

$$g_{\uparrow\downarrow}(\gamma \rightarrow 0, z=0) = 1 - \frac{3}{\pi^2} g_v \gamma + O(\gamma^2), \quad (25b)$$

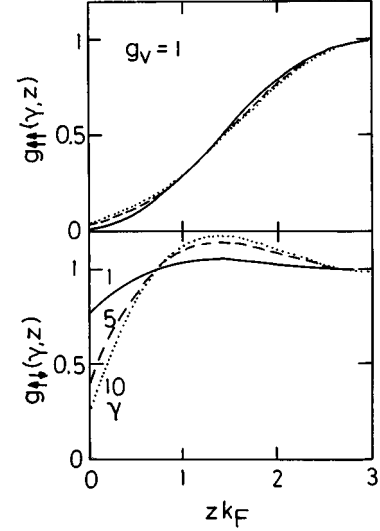


FIG. 8. Pair-correlation functions $g_{\uparrow\uparrow}(\gamma, z)$ and $g_{\uparrow\downarrow}(\gamma, z)$ vs distance z according to Eq. (24) for $\gamma = 1, 5$, and 10 as solid, dashed, and dash-dotted lines, respectively.

which corresponds to $g_{\uparrow\uparrow}(\gamma \rightarrow 0, z=0) = 0.0257\gamma^2$ and $g_{\uparrow\downarrow}(\gamma \rightarrow 0, z=0) = 1 - 0.304\gamma$ for $g_v = 1$. For strong coupling we find

$$g_{\uparrow\uparrow}(\gamma \rightarrow \infty, z=0) = \frac{\pi^2}{8\gamma} [1 - 2/g_v^2 + (1 + 2/g_v^2)^{1/2}] \quad (26a)$$

and

$$g_{\uparrow\downarrow}(\gamma \rightarrow \infty, z=0) = \frac{\pi^2}{8\gamma} [1 + (1 + 2/g_v^2)^{1/2}], \quad (26b)$$

which corresponds to $g_{\uparrow\uparrow}(\gamma \rightarrow \infty, z=0) = 0.903/\gamma$ and $g_{\uparrow\downarrow}(\gamma \rightarrow \infty, z=0) = 3.37/\gamma$ for $g_v = 1$. Numerical results for $g_{\uparrow\uparrow}(\gamma, z)$ and $g_{\uparrow\downarrow}(\gamma, z)$ versus z are shown in Fig. 8 for $\gamma = 1, 5$, and 10 . The exchange hole and the Coulomb hole can be clearly seen. The strength of the interaction only modifies the pair-correlation function $g_{\uparrow\downarrow}(\gamma, z)$ for $zk_F < 1.5$. $g_{\uparrow\uparrow}(\gamma, z)$ is nearly insensitive to the strength of the interaction. More detailed results for $g_{\uparrow\uparrow}(\gamma, z \rightarrow \infty)$ and $g_{\uparrow\downarrow}(\gamma, z \rightarrow \infty)$ are given in Sec. VI.

C. Paramagnetic spin susceptibility

The static paramagnetic spin susceptibility $\mathbf{X}_s(q) = \mathbf{X}_s(q, \omega=0)$ is given by

$$\mathbf{X}_s(q) = \frac{\mathbf{X}_0(q)}{1 - V_0 G_s(\gamma) \mathbf{X}_0(q)}. \quad (27)$$

For the spin susceptibility in the long-wavelength limit, we obtain

$$\mathbf{X}_s(q \rightarrow 0) / \rho_F = \frac{1}{1 - 4g_v^2 \gamma G_s(\gamma) / \pi^2}. \quad (28)$$

For small coupling ($\gamma \rightarrow 0$) we derive $\mathbf{X}_s(q \rightarrow 0) / \rho_F = 1 + 2g_v \gamma / \pi^2 - 2g_v^2 \gamma^2 / \pi^4$. The term γ^2 represents correlation effects and reduces the spin susceptibility. For large

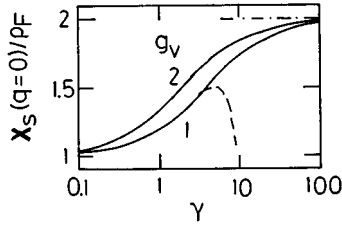


FIG. 9. Paramagnetic spin susceptibility $\mathbf{X}_s(q \rightarrow 0)$ vs interaction strength γ according to Eq. (28) for $g_v=1$ and 2. The dashed and dash-dotted lines correspond to the asymptotic results.

coupling ($\gamma \rightarrow \infty$) we obtain $\mathbf{X}_s(q \rightarrow 0)/\rho_F = 2$. Note that the strong-coupling behavior is independent of the valley degeneracy, while for weak coupling the exchange term increases with increasing valley degeneracy.

Numerical results for the paramagnetic spin susceptibility versus γ are shown in Fig. 9 together with the asymptotic results. We mention that, with increasing valley degeneracy, $\mathbf{X}_s(q \rightarrow 0)$ increases; however, the dependence is small.

D. Density waves and spin waves

The dispersion of the collective modes is given by the poles of the response functions. With the LFC the dispersion of the collective modes for density fluctuations $\omega_d(q)$, and for spin fluctuations $\omega_s(q)$ is expressed as

$$\frac{\omega_{d,s}(q)}{\epsilon_F} = 2 \frac{|q|}{k_F} \left[\frac{B_+(q)^2 A_{d,s}(q) - B_-(q)^2}{A_{d,s}(q) - 1} \right]^{1/2}, \quad (29)$$

with

$$A_d(q) = \exp[\pi^2 |q| / (2k_F g_v^2 \gamma [1 - G(\gamma)])] \quad (30a)$$

and

$$A_s(q) = \exp[-\pi^2 |q| / (2k_F g_v^2 \gamma G_s(\gamma))]. \quad (30b)$$

Equation (29) was first derived in Ref. 19 for density modes. Note that $B_{\pm}(q) = 1 \pm |q|/2k_F$ describes the electron-hole (eh) spectrum via $\omega_{\pm \text{eh}}/\epsilon_F = 2|q| |B_{\pm}(q)|/k_F$. The electron-hole spectrum ω_{eh} is characterized by $\omega_{-\text{eh}} \leq \omega_{\text{eh}} \leq \omega_{+\text{eh}}$. For small wave numbers one finds $\omega_{+\text{eh}} = \omega_{-\text{eh}} = 2\epsilon_F |q|/k_F \propto |q|$, and collective modes with the dispersion of a sound mode: $\omega_{d,s}(q \rightarrow 0) \propto |q|$.

The dispersion for the collective modes versus wave number is shown in Fig. 10 for $\gamma=10$ and for (a) small wave numbers $0 < q < 0.5k_F$, where $\omega_s(q) < \omega_{\text{eh}\pm}(q) < \omega_d(q)$, and (b) large wave numbers $q \approx 2k_F$, where $\omega_s(q)$ for $1.97 < q/k_F < 2.03$ is overdamped but reappears for $q < 1.97k_F$ and $q > 2.03k_F$. This behavior can be understood as follows: for $q = 2k_F$ we find $B_+ = 2$ and $B_- = 0$ and $\omega_{d,s}/\epsilon_F = 8A_{d,s}^{1/2}/[A_{d,s} - 1]^{1/2}$. For spin waves the parameter $A_s(q)$ is characterized by $0 < A_s(q) < 1$, and spin modes are overdamped: $\omega_s(2k_F)/\epsilon_F = i\Gamma$, with $\Gamma = 8A_s(2k_F)^{1/2}/[1 - A_s(2k_F)]^{1/2}$. We suggest that such a behavior can be seen in experiment. For $\gamma \rightarrow 0$ $A_s(2k_F)$ is exponentially small. The wave numbers q_1 and q_2 , where $\omega_s(q_1 < |q| \approx 2k_F < q_2)$ is imaginary, are given by $|q_{1,2}|/2k_F = 1 \pm 2 \exp[-\pi^2 / [2g_v^2 \gamma G_s(\gamma)]]$. For $\gamma \rightarrow 0$ we obtain $|q_{1,2}| = 2k_F [1 \pm 2 \exp(-\pi^2/g_v \gamma)]$, and for $\gamma \rightarrow \infty$ we derive $|q_{1,2}|$

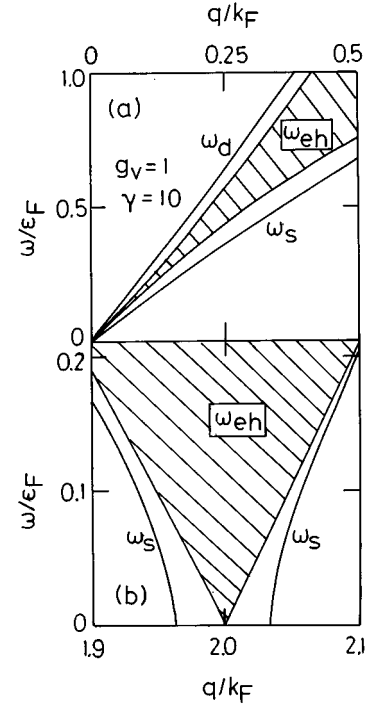


FIG. 10. $\omega_d(q)$, $\omega_s(q)$, and $\omega_{\text{eh}\pm}(q)$ vs wave number q for $\gamma=10$ according to Eqs. (29) and (30) for (a) $q \leq 0.5k_F$ and (b) $1.9k_F \leq q \leq 2.1k_F$. The shaded area represents the electron-hole excitation spectrum.

$= 2k_F [1 \pm 0.0366]$. For density waves [not shown in Fig. 10(b)] the parameter A_d fulfills $A_d(q) > 1$ and no anomalies are seen for $q \approx 2k_F$.

In the long-wavelength limit the collective modes are well defined. We find the analytical results

$$\frac{\omega_d(q \rightarrow 0)}{\omega_{\text{eh}\pm}(q \rightarrow 0)} = \left[1 + \frac{4g_v^2}{\pi^2} \gamma [1 - G(\gamma)] \right]^{1/2} \quad (31a)$$

and

$$\frac{\omega_s(q \rightarrow 0)}{\omega_{\text{eh}\pm}(q \rightarrow 0)} = \left[1 - \frac{4g_v^2}{\pi^2} \gamma G_s(\gamma) \right]^{1/2}. \quad (31b)$$

For weak coupling we obtain $\omega_d(q \rightarrow 0)/\omega_{\text{eh}\pm}(q \rightarrow 0) = [1 + 2g_v \gamma (2g_v - 1)/\pi^2]^{1/2} > 1$ and $\omega_s(q \rightarrow 0)/\omega_{\text{eh}\pm}(q \rightarrow 0) = [1 - 2g_v \gamma/\pi^2]^{1/2} < 1$: for $\gamma \rightarrow 0$ the energies for the two collective modes approach the energy of the electron-hole excitations. For $g_v=1$ we find $\omega_d(q \rightarrow 0) = (v_F + V_0/2\pi)q$ and $\omega_s(q \rightarrow 0) = (v_F - V_0/2\pi)q$, and v_F is the Fermi velocity. This result is in agreement with the ‘‘g-ology’’ method.¹⁸

For strong coupling we obtain $\omega_d(q \rightarrow 0)/\omega_{\text{eh}\pm}(q \rightarrow 0) = [1 + g_v^2 \delta/2]^{1/2} > 1$ and $\omega_s(q \rightarrow 0)/\omega_{\text{eh}\pm}(q \rightarrow 0) = \frac{1}{2}^{1/2} < 1$, and we conclude that in the strong-coupling limit the collective modes are well defined. Our results can be summarized by $\omega_s(q \rightarrow 0) < \omega_{\text{eh}\pm}(q \rightarrow 0) < \omega_d(q \rightarrow 0)$. For weak coupling we obtain $\omega_d(q \rightarrow 0)/\omega_s(q \rightarrow 0) = 1 + 2g_v^2 \gamma/\pi^2$, and for strong coupling $\omega_d(q \rightarrow 0)/\omega_s(q \rightarrow 0) = [2 + \delta g_v^2]^{1/2}$. Numerical results for $\omega_d(q \rightarrow 0)/\omega_{\text{eh}\pm}(q \rightarrow 0)$ and $\omega_s(q \rightarrow 0)/\omega_{\text{eh}\pm}(q \rightarrow 0)$ versus γ are shown in Fig. 11 for $g_v=1$. With increasing γ the different modes become well separated in energy: this is called spin-charge separation.

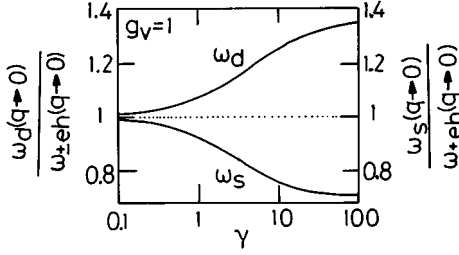


FIG. 11. Long-wavelength limit of $\omega_d(q \rightarrow 0)/\omega_{\text{eh}\pm}(q \rightarrow 0)$ and $\omega_s(q \rightarrow 0)/\omega_{\text{eh}\pm}(q \rightarrow 0)$ vs interaction strength γ according to Eq. (31).

With increasing valley degeneracy $\omega_d(q \rightarrow 0)/\omega_{\text{eh}\pm}(q \rightarrow 0)$ increases strongly, while $\omega_s(q \rightarrow 0)/\omega_{\text{eh}\pm}(q \rightarrow 0)$ decreases. However, the dependence on the valley degeneracy is less pronounced for the spin modes if compared to the density modes. This is due to the fact that even for $g_v \rightarrow \infty$ the relation $\omega_s(q \rightarrow 0)/\omega_{\text{eh}\pm}(q \rightarrow 0) > 0.707$ applies.

V. DISCUSSION: THEORY

A. STLS and LST approaches

In this paper many-body effects for density and spin correlations have been discussed within the concept of the LFC for the one-dimensional electron gas with a short-range interaction potential. The methods of STLS (Ref. 3) and LST (Ref. 13) have been used. It is known^{2,3,13,19} that these methods are not exact. However, it is generally accepted that these methods give qualitatively correct results even for intermediate coupling. The comparison of the ground-state energy calculated within the STLS approach with exact results⁵ showed that the weak-coupling limit is exact, and reasonable agreement was found for intermediate coupling.

For a Bose gas it was found that the ground-state energy within the RPA for the LFC [which corresponds to Eq. (12) for $1/g_v = 0$] gives wrong results for $\gamma > 2$,²⁰ while the collective density modes calculated within the same approximation are in good agreement with exact results for $\gamma < 10$.²⁴ For the Bose gas and $1/\gamma = 0$, one can show that the sound velocity calculated within the STLS approach is a factor 2 lower than the exact result. It was noted before that to reach the strong-coupling regime the parameter γ must be large, $\gamma > 37$.²⁰ We believe that similar results apply to the electron gas, where, however, exact results for the density modes are not available in the literature. We expect that our quasianalytical results within the STLS and LST approaches are quantitatively correct for $\gamma < 10$, and can be used to estimate many-body effects. For $\gamma > 10$, qualitative aspects of many-body effects can be deduced from our results. The STLS approach was used²⁵ to calculate the ground-state energy of the Hubbard model, and was found to be in good agreement with exact results.

In general, the LFC $G(q, \omega)$ is a function of the wave number q and of the frequency ω . In the STLS approach the frequency dependence is neglected, and it was shown that $G_{\text{STLS}}(q) = G(q, \omega \rightarrow \infty)$.¹⁹ One motivation for the present paper was (i) to obtain analytical results which can be used by experimenters to estimate the importance of many-body effects, and (ii) to test the analytical form of the SSF. Our

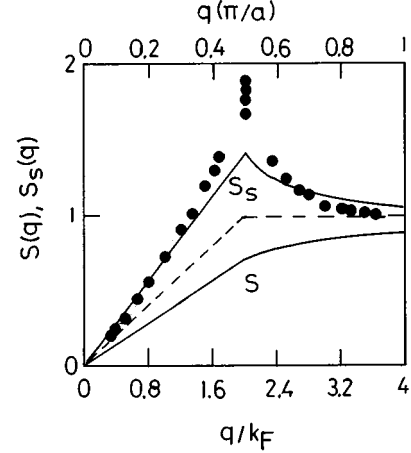


FIG. 12. Static-structure factor for charge fluctuations $S(q)$ and spin fluctuations $S_s(q)$ vs wave number q in the strong-coupling limit $\gamma \rightarrow \infty$. The solid dots are numerical results for the Hubbard model (Ref. 29).

results concerning the valley degeneracy represent a generalization of the STLS and LST approaches. The model of a short-range interaction potential leads, with the analytical form of the SSF, to *analytical* results concerning the density response function and the spin response function, and these results depend in a nontrivial way on the strength parameter γ and the valley degeneracy g_v .

A similar form of the SSF for charge fluctuations was discussed before in connection with a two-dimensional electron gas.²⁶ The analytical form of the SSF was recently applied to an electron gas with long-range Coulomb interaction.²⁷ The nonanalytical contribution of correlation effects to the ground-state energy in three- and two-dimensional electron gases was obtained, in good agreement with results from the literature.

The STLS and LST approaches do not fulfill the compressibility sum rule.^{2,5} A theory fulfilling this sum rule and containing the frequency dependence of the LFC was formulated²⁸ for a three-dimensional electron gas with long-range Coulomb interaction. It is clear that the present approach should be generalized following the approach of Ref. 28. We believe, however, that within such a more general approach only numerical results can be obtained.

B. Strong-coupling limit: $\gamma \rightarrow \infty$

While our theory is a weak-coupling theory, and exact for $\gamma \rightarrow 0$, it is interesting to note that reasonable results are obtained for $\gamma \rightarrow \infty$. For instance, for $g_v = 1$ we obtain the strong-coupling limit for the SSF for charge fluctuations as $S(q < 2k_F) = 0.366q/k_F$ and $S(q > 2k_F) = 1/(1 + 3.46k_F^2/q^2)^{1/2}$. For spin fluctuations we find $S_s(q < 2k_F) = 0.707q/k_F$ and $S_s(q > 2k_F) = 1/(1 - 2k_F^2/q^2)^{1/2}$. We note $S(q < 2k_F)$ and $S_s(q < 2k_F)$ are linear in q , and $S_s(q = 2k_F)$ exhibits a peak at $q = 2k_F$.

Our strong-coupling results for $\gamma \rightarrow \infty$ and $g_v = 1$ are shown in Fig. 12 together with recent numerical results²⁹ for the spin-spin correlation function of the Hubbard model in the strong-coupling limit $U/t = 10^3$, where t is the parameter for the kinetic energy and U the parameter for the interac-

tion. The peak value which we find for spin fluctuations [$S_s(q=2k_F)=1.41$] is smaller than in the Hubbard model [$S_s(q=2k_F)\approx 1.8$].^{29,30} The comparison with the Hubbard model and the fact that $S_s(q=2k_F)$ is finite for $\gamma\rightarrow\infty$ indicates that $G_s(\gamma)\propto 1/\gamma$. We believe that the numerical differences seen in Fig. 12 are due to differences in the models. We mention that an increase of the *prefactor* in the strong-coupling result in Eq. (22) by 35% would increase our peak value to 1.8. It is astonishing, due to the appearance of a minus sign in Eq. (16), that within our theory $S_s(q)$ exists in the limit $\gamma\rightarrow\infty$. We also note that for $q\rightarrow 0$ we find very good agreement between our result $S_s(q<2k_F)=0.707q/k_F$ and the numerical results; see Fig. 12: this is not trivial because $S_s(q<2k_F)$ is determined by $S_0(q)$ (factor 4) and $G_s(\gamma\rightarrow\infty)$ (factor -2).

For the collective modes we find, for $\gamma\rightarrow\infty$,

$$\omega_d(q\rightarrow 0)=1.35v_Fq \quad (32a)$$

and

$$\omega_s(q\rightarrow 0)=0.71v_Fq. \quad (32b)$$

Within the Hubbard model one obtains for $U/t\rightarrow\infty$ $\omega_d(q\rightarrow 0)=2tq$ and for a quarter-filled band with band-filling parameter $n_b=0.5$ and with $v_F=2t\sin(\pi n_b/2)$ one finds $v_F=2^{1/2}t$ and $\omega_d(q\rightarrow 0)=2^{1/2}v_Fq$.^{31,32} This is in good agreement with our result. For the Hubbard model the strong-coupling result is given by $\omega_s(q\rightarrow 0)/q\propto t^2/U$, which means that $\omega_s(q\rightarrow 0)/q=\pi 2^{1/2}(t/U)v_F$,^{33,31} and the energy of the spin modes goes to zero for $U/t\rightarrow\infty$. This is in disagreement with our result and might be due to the different models.

C. Comparison with the Hubbard model

The Luttinger liquid and the Hubbard model in one dimension can be solved exactly.^{15,34,35} It is difficult to compare our results with results for the spin susceptibility,³⁶ the density susceptibility,³⁷ the spin-spin correlation function,^{29,30} spin-density waves,^{31,33} density waves,^{31,32} and correlation functions^{16,17,38} obtained for the Hubbard model: the Hubbard model is a lattice model with a length scale a , and all wave numbers are restricted to $0\leq q\leq\pi/a$. Our model is a continuum model with $0\leq q<\infty$. Therefore, for the spin-spin correlation function [see Fig. 12], a real comparison for $q>2k_F$ is impossible. Moreover, the dispersion relation for the kinetic energy within the two models is different, which makes a correct identification of the parameters difficult. Within bosonization techniques¹⁶ and the conformal field theory,¹⁷ an additional approximation is used: linearization of the kinetic energy at the Fermi energy. We work with a parabolic dispersion relation. It was argued that the one-dimensional interacting fermion problem with *nonlinear* dispersion can be treated in terms of the RPA with a LFC included.³⁹ This argument shows that the LFC is an important issue in order to study many-body effects in systems with parabolic dispersion.

For small wave numbers we find the following relations:

$$\omega_d(q)/v_Fq=[\rho_F/\mathbf{X}(q)]^{1/2} \quad (33a)$$

and

$$\omega_s(q)/v_Fq=[\rho_F/\mathbf{X}_s(q)]^{1/2}. \quad (33b)$$

This behavior is a consequence of $\mathbf{X}_0(q,\omega\rightarrow\infty)\propto q^2/\omega^2$, and the structure of our response functions as given in Eq. (2) for $\mathbf{X}(q,\omega)$, and in Eq. (16) for $\mathbf{X}_s(q,\omega)$. Within the Hubbard model similar results to those in Eq. (33) have been obtained as approximating results for density waves and spin waves using sum-rule arguments:⁴⁰ it is fair to say that for the Hubbard model in the weak-coupling limit the collective modes are well described by an equation equivalent to Eq. (33). However, it is clear from Ref. 40, that, for the Hubbard model, Eq. (33) is only valid at weak coupling. An exact relation exists between $\omega_d(q)$ and $\mathbf{X}(q)$,¹⁷ and also between $\omega_s(q)$ and $\mathbf{X}_s(q)$.^{31,32}

D. Overdamped spin modes at $q\approx 2k_F$

A recent Monte Carlo simulation for the one-dimensional Hubbard model⁴¹ showed, in the case of doping, collective density and spin excitations in qualitative agreement with our results. It was found that at $q\approx 2k_F$ the energy of the spin mode becomes very small. This result is in qualitative agreement with our calculation: see Fig. 10(b). The overdamping of the spin mode near $q=2k_F$ was not seen due to accuracy problems of 10% near this wave number. In fact, Eq. (29) describes analytically the dispersion of spin waves.

For small wave numbers it was reported⁴¹ that the sound velocity v_n of the density mode is larger than the sound velocity v_s of the spin mode ($v_n/v_s=1.5$). This is in qualitative agreement with our results. For $g_v=1$ we find $1<v_n/v_s<1.93$ for $0<\gamma<\infty$. The behavior $v_n/v_s>1$ is called the spin charge separation in the current literature. In the lattice model the one-particle excitations have been described as cosinelike bands,⁴¹ while in our model the dispersion is parabolic. We conclude that the excitation spectrum in the doped Hubbard model shows features similar to those of the excitation spectrum in our model.

VI. CRITICAL EXPONENTS AND THE LOCAL-FIELD CORRECTION

A. Long-distance behavior of $g(\gamma,z)$

In a recent paper⁹ about the LFC of a Bose condensate, we showed that the pair-correlation function is given by the LFC via

$$g(\gamma,z\rightarrow\infty)=1-\pi/2(zn\pi)^2\gamma^{1/2}[1-G(\gamma)]^{1/2}. \quad (34a)$$

Following the arguments given in Ref. 16, we write

$$g(\gamma,z\rightarrow\infty)=1-K(\gamma)/(\pi n z)^2, \quad (34b)$$

and this relation holds for electron (E) with $K(\gamma)=K_E(\gamma)$ and for bosons (B) with $K(\gamma)=K_B(\gamma)$ in one dimension. The critical coefficient $K(\gamma)$ determines the long-distance decay of correlation functions in one dimensional systems. Sometimes one uses K_ρ (Ref. 32) or η (Ref. 16) in the literature instead of $K(\gamma)$. We conclude that for the Bose condensate and with the concept of a LFC, the relation

$$K_B(\gamma)=\pi/[2\gamma^{1/2}[1-G(\gamma)]^{1/2}] \quad (35a)$$

holds. If we used the STLS result $G(\gamma) = 2\gamma^{1/2}[1 - G(\gamma)]^{1/2}/\pi$ (Ref. 9) with $G(\gamma) = 2\gamma[(1 + \pi^2/\gamma)^{1/2} - 1]/\pi^2$ we find

$$K_B(\gamma) = 1/G(\gamma). \quad (35b)$$

This is a quite remarkable result: many-body effects described by the LFC determine the long-distance behavior of correlation functions described by $K(\gamma)$. We note that for a Bose gas in one dimension $G(\gamma \rightarrow 0) = 2\gamma^{1/2}/\pi$ and $G(\gamma \rightarrow \infty) = 1 - \pi^2/4\gamma$,⁹ and it follows that $K_B(\gamma \rightarrow 0) = \pi/2\gamma^{1/2}$ and $K_B(\gamma \rightarrow \infty) = 1 + \pi^2/4\gamma$. For a Bose condensate, $K_B(\gamma) \rightarrow \infty$ diverges for $\gamma \rightarrow 0$.¹⁶

B. Electron gas

In general $K(\gamma)$ is calculated by renormalization-group techniques or via the conformal field theory. For long-range interaction many-body effects are described by the LFC, which can be calculated within the STLS approach. Our observation described above indicates (i) that $K(\gamma)$ is given by the LFC, and this closes the theoretical gap between these two approaches; and (ii) that the STLS and LST approaches can be used to obtain estimates for the LFC's and determine, therefore, the critical coefficients.

For the Hubbard model some critical exponents have been calculated within the conformal field theory:^{17,32,42,43} $0.5 \leq \eta \leq 1$ for the density-density correlation function, $1 \leq \gamma \leq 2$ for the spin-spin correlation function, $0 \leq \alpha \leq 1/8$ for the momentum-distribution function, and $2 \leq \beta \leq 4$ for $4k_F$ oscillations in the density-density correlation function. These critical exponents depend on the interaction strength (U/t) and the band-filling parameter n_b .

In order to calculate $K_E(\gamma)$ for the one-dimensional electron gas, we have to calculate $g(\gamma, z \rightarrow \infty)$. For the free-electron gas we obtain the exact result

$$g_{\text{HFA}}(z) = 1 - \frac{g_v}{(\pi n z)^2} [1 - \cos(2k_F z)], \quad (36)$$

with $g_{\text{HFA}}(z=0) = 1 - 1/2g_v$. With Eq. (9) we find

$$g(\gamma, z \rightarrow \infty) = 1 - \frac{K_E(\gamma)}{(z n \pi)^2} \left[1 - \frac{K_E(\gamma^2)}{g_v^2} \cos(2k_F z) + O(1/z^2) \right], \quad (37)$$

with

$$K_E(\gamma) = \frac{g_v}{[1 + 4g_v^2\gamma[1 - G(\gamma)]/\pi^2]^{1/2}}. \quad (38)$$

$K_E(\gamma)$ determines the long-distance decay of the pair-correlation function. We note that $g(\gamma, z) \propto \langle n(z)n(0) \rangle$ describes the density-density correlation function. For $\gamma=0$ we find $K_E(\gamma=0) = g_v$, and Eq. (37) becomes identical to Eq. (36). We note that we did not find the $4k_F$ oscillations discussed recently in the literature for the Hubbard model.^{16,32} In the weak-coupling limit we find $K_E(\gamma \rightarrow 0) = g_v/[1 + 4g_v^2\gamma[1 - 1/2g_v]/\pi^2]^{1/2}$, and for strong coupling $K_E(\gamma \rightarrow \infty) = g_v/[1 + g_v^2\delta/2]^{1/2}$. For $g_v=1$ we derive the weak-coupling result as $K_E(\gamma \rightarrow 0) = 1/[1 + 2\gamma/\pi^2]^{1/2} \approx 1 - \gamma/\pi^2$

$= 1 - V_0/2\pi v_F$ and the strong-coupling result as $K_E(\gamma \rightarrow \infty) = 1/[1 + 1.73/2]^{1/2} = 0.73$. For the Hubbard model one finds $K_E(U/t \rightarrow 0) = 1 - U/\pi v_F$ and $K_E(U/t \rightarrow \infty) = 0.5$.³²

With $K_E(\gamma)$ the singularity in the momentum distribution function is written as^{17,32,42}

$$n(k) = 0.5 - \text{const} \text{sgn}(k - k_F) |k - k_F|^\alpha, \quad (39)$$

with $\alpha = [K_E(\gamma)/g_v + g_v/K_E(\gamma) - 2]/4$. The density of states the $\rho(\epsilon)$ near the Fermi energy is expressed $\rho(\epsilon) \approx |\epsilon - \epsilon_F|^\alpha$. For $g_v=1$ we find in the weak-coupling limit $\alpha = \gamma^2/4\pi^2$ and within the strong-coupling limit we obtain $\alpha = 0.025$. We conclude that $0 \leq \alpha \leq 0.025$, while in the Hubbard model $0 \leq \alpha \leq 0.125$.

For the spin correlations one has to calculate $g_s(\gamma, z \rightarrow \infty)$. For the free-electron gas we obtain the exact result

$$g_{s,\text{HFA}}(z) = \frac{g_v}{(\pi n z)^2} [1 - \cos(2k_F z)], \quad (40)$$

with $g_{s,\text{HFA}}(z=0) = 1/2g_v$. With Eq. (23), we find

$$g_s(\gamma, z \rightarrow \infty) = \frac{K_{E,s}(\gamma)}{(z n \pi)^2} \left[1 - \frac{K_{E,s}(\gamma)^2}{g_v^2} \cos(2k_F z) + O(1/z^2) \right], \quad (41)$$

with

$$K_{E,s}(\gamma) = \frac{g_v}{[1 - 4g_v^2\gamma G_s(\gamma)/\pi^2]^{1/2}}. \quad (42)$$

Note, that it is $G_s(\gamma)$ which determines $K_{E,s}(\gamma)$. From our results for $G_s(\gamma)$ we find $K_{E,s}(\gamma \rightarrow 0) = g_v/[1 - 2g_v\gamma/\pi]^{1/2}$ and $K_{E,s}(\gamma \rightarrow \infty) = 2^{1/2}g_v$.

It is easy to calculate the behaviors of $g_{\uparrow\downarrow}(\gamma, z \rightarrow \infty)$ and $g_{\uparrow\uparrow}(\gamma, z \rightarrow \infty)$, which are determined by $K_{E,\uparrow\downarrow}(\gamma) = [K_E(\gamma) + K_{E,s}(\gamma)]/2$ and $K_{E,\uparrow\uparrow}(\gamma) = [K_E(\gamma) - K_{E,s}(\gamma)]/2$, respectively. For $g_v=1$ the weak-coupling results are given by $K_{E,\uparrow\downarrow}(\gamma \rightarrow 0) = 1 + 3\gamma^2/\pi^4$ and $K_{E,\uparrow\uparrow}(\gamma \rightarrow 0) = -\gamma/\pi^2$, while for strong coupling we derive $K_{E,\uparrow\downarrow}(\gamma \rightarrow \infty) = 1.073$ and $K_{E,\uparrow\uparrow}(\gamma \rightarrow \infty) = -0.34$.

VII. DISCUSSION: EXPERIMENTS

It was shown that for quantum wires based on doped GaAs, the energy ordering of the elementary excitations follows $\omega_d(q) > \omega_{\text{eh}\pm}(q) > \omega_s(q)$ with $\omega_d(q) \approx 2.5\omega_{\text{eh}\pm}(q)$ and $\omega_s(q) \approx 0.8\omega_{\text{eh}\pm}(q)$ for $0.037 \leq q/k_F \leq 0.11$.⁴⁴ Our results are in qualitative agreement with these experimental findings: see Fig. 10(a). In our calculations we neglected the long-range character of the interaction potential (the Coulomb interaction^{5,45}), which is present in these structures. Therefore, only qualitative agreement of our theory with the experimental results reported in Ref. 44 can be expected. In a recent paper,⁴⁶ it was shown that in quasi-one-dimensional systems, based on doped GaAs, the spin-density excitations show a linear dispersion with $\omega_s(q) \approx \omega_{\text{eh}\pm}(q)$, which is in agreement with our theory if γ is small.

Interacting electron gases are often discussed within the

mean-field approach for $\mathbf{X}(q, \omega)$, which corresponds to $G(\gamma) = 0$, and the Stoner approach for $\mathbf{X}_s(q, \omega)$,⁴⁷ which corresponds to $G_{s,\text{HFA}} = 1/2g_v$: many-body effects are neglected for the density susceptibility, and overestimated for the spin susceptibility. For instance, if the HFA is used for $\mathbf{X}_s(q)$ to estimate many-body effects for the paramagnetic spin susceptibility, one obtains $\mathbf{X}_s(q \rightarrow 0)/\rho_F = 1.81$ for $\gamma = 4$ and $g_v = 1$, while the LST approach gives $\mathbf{X}_s(q \rightarrow 0)/\rho_F = 1.50$; see Fig. 9. If, in experiment, $\mathbf{X}_s(q \rightarrow 0)/\rho_F = 1.5$ is measured, we deduce from the HFA for $\mathbf{X}_s(q \rightarrow 0)/\rho_F$ the value $\gamma = 2.46$ while the full LST approach implies $\gamma = 4$; see Fig. 9. These estimates demonstrate the power of our approach. We expect that our results are interesting for experimenters working with one-dimensional systems as realized in organic materials, and for experimenters working with artificial one-dimensional systems made with GaAs/Al_xGa_{1-x}As heterostructures.

VIII. CONCLUSION

In this paper we discussed many-body effects for a one-dimensional electron gas with short-range interaction via the random-phase approximation and the concept of the local-field correction $G(\gamma)$. The comparison of our results by using an analytical expression for the SSF with the STLS approach, where numerical results for the SSF are used, shows that the analytical form of the SSF is a good approximation of the real SSF. This implies that the generalized Feynman-Bijl approach for the SSF could be useful for model potentials which cannot be solved exactly, as for instance in systems with dimension larger than one.

With the analytical results given in this paper for the local-field correction $G(\gamma)$, the pair-correlation function, and the ground-state energy of a one-dimensional electron gas with a short-range interaction we have demonstrated: Hartree, exchange and correlation effects depend in a non-trivial way on the strength parameter γ and the valley degeneracy g_v . We also discussed spin correlations with the concept of the local-field correction $G_s(\gamma)$. The analytical results for the paramagnetic susceptibility and the collective modes describe spin correlations in a one-dimensional electron gas with short-range interaction.

It was shown that local-field corrections describe the critical exponents of the long-distance behavior of the density-density and the spin-spin correlation functions. This observation gives some insight into the ‘‘theoretical’’ gap between conformal field theories and the renormalization group on the one hand, and the concept of a local-field correction on the other hand.

Our results show that the excitation spectrum in our model (one-particle excitations, density excitations, and spin excitations) is similar to the excitation spectrum of the doped Hubbard model. We found that spin waves become overdamped at $q \approx 2k_F$.

ACKNOWLEDGMENTS

The ‘‘Laboratoire de Physique des Solides’’ is a ‘‘Laboratoire associé au Centre National de la Recherche Scientifique (CNRS).’’

-
- ¹D. Pines and P. Nozières, *The Theory of Quantum Liquids* (Benjamin, New York, 1966), Vol. I.
- ²G. D. Mahan, *Many-Particle Physics* (Plenum, New York, 1990).
- ³K. S. Singwi, M. P. Tosi, R. H. Land, and A. Sjölander, *Phys. Rev.* **176**, 589 (1968).
- ⁴C. N. Yang, *Phys. Rev. Lett.* **19**, 1312 (1967).
- ⁵W. I. Friesen and B. Bergersen, *J. Phys. C* **13**, 6627 (1980).
- ⁶A. Gold, *Z. Phys. B* **89**, 1 (1992).
- ⁷A. Gold and L. Calmels, *Phys. Rev. B* **48**, 11 622 (1993).
- ⁸A. Gold, *Phys. Rev. B* **50**, 4297 (1994).
- ⁹A. Gold, *Z. Phys. B* **91**, 397 (1993).
- ¹⁰D. Többen, D. A. Wharam, G. Abstreiter, and J. P. Kotthaus, *Phys. Rev. B* **52**, 4704 (1995).
- ¹¹D. Q. Jin, J. R. Ensher, M. P. Matthews, C. E. Wiemann, and E. A. Cornell, *Phys. Rev. Lett.* **77**, 420 (1996); M. O. Mewes, M. R. Andrews, N. J. van Druten, D. M. Kurn, D. S. Durfee, C. G. Townsend, and W. Ketterle, *Phys. Rev. Lett.* **77**, 988 (1996).
- ¹²W. Ketterle and N. J. van Druten, *Phys. Rev. A* **54**, 656 (1996).
- ¹³R. Lobo, K. S. Singwi, and M. P. Tosi, *Phys. Rev.* **186**, 470 (1969).
- ¹⁴G. Senatore and N. H. March, *Rev. Mod. Phys.* **66**, 445 (1994).
- ¹⁵D. C. Mattis, *The Many-Body Problem* (World Scientific, Singapore, 1993); E. B. Kolomeisky and J. P. Straley, *Rev. Mod. Phys.* **68**, 175 (1996).
- ¹⁶F. D. M. Haldane, *Phys. Rev. Lett.* **47**, 840 (1981).
- ¹⁷H. Frahm and V. E. Korepin, *Phys. Rev. B* **42**, 10 553 (1990).
- ¹⁸J. Solyom, *Adv. Phys.* **28**, 201 (1979).
- ¹⁹S. Nagano and K. S. Singwi, *Phys. Rev. B* **27**, 6732 (1983).
- ²⁰E. H. Lieb and W. Lininger, *Phys. Rev.* **130**, 1605 (1963).
- ²¹M. Girardeau, *J. Math. Phys.* **1**, 516 (1960).
- ²²A. Ishihara, in *Solid State Physics*, edited by H. Ehrenreich and D. Turnbull (Academic, New York, 1989), Vol. 42.
- ²³A. Gold and L. Calmels, *Philos. Mag. Lett.* **74**, 33 (1996).
- ²⁴E. H. Lieb, *Phys. Rev.* **130**, 1616 (1963).
- ²⁵M. R. Hedyati and G. Vignale, *Phys. Rev. B* **40**, 9044 (1989).
- ²⁶B. Tanatar and D. M. Ceperley, *Phys. Rev. B* **39**, 5005 (1989); B. Tanatar, *Phys. Lett. A* **158**, 153 (1991).
- ²⁷A. Gold and L. Calmels, *Solid State Commun.* **96**, 101 (1995).
- ²⁸C. F. Richardson and N. W. Ashcroft, *Phys. Rev. B* **50**, 8170 (1994).
- ²⁹S. Qin, S. Liang, Z. Su, and L. Yu, *Phys. Rev. B* **52**, R5475 (1995).
- ³⁰M. Ogata and H. Shiba, *Phys. Rev. B* **41**, 2326 (1990).
- ³¹C. F. Coll, *Phys. Rev. B* **9**, 2150 (1974).
- ³²H. J. Schulz, *Phys. Rev. Lett.* **64**, 2831 (1990).
- ³³A. A. Ovchinnikov, *Zh. Eksp. Teor. Fiz.* **57**, 2137 (1969) [*Sov. Phys. JETP* **30**, 1160 (1970)]; M. Takahashi, *Prog. Theor. Phys.* **43**, 1619 (1970).
- ³⁴D. C. Mattis and E. H. Lieb, *J. Math. Phys.* **6**, 304 (1965).
- ³⁵E. H. Lieb and F. Y. Wu, *Phys. Rev. Lett.* **20**, 1445 (1968).
- ³⁶H. Shiba, *Phys. Rev. B* **6**, 930 (1972).
- ³⁷T. Usuki, N. Kawakami, and A. Okiji, *Phys. Lett. A* **135**, 476 (1989).

- ³⁸C. C. Gearhart and J. C. Hicks, Phys. Rev. B **52**, 7787 (1995).
- ³⁹P. Kopietz, J. Hermisson, and K. Schönhammer, Phys. Rev. B **52**, 10 877 (1995).
- ⁴⁰T. Momoi, Phys. Lett. A **195**, 351 (1994).
- ⁴¹R. Preuss, A. Muramatsu, W. von der Linden, P. Dieterich, F. F. Assaad, and W. Hanke, Phys. Rev. Lett. **73**, 732 (1994).
- ⁴²A. Parola and S. Sorella, Phys. Rev. Lett. **64**, 1831 (1990).
- ⁴³N. Kawakami and S. K. Yang, Phys. Lett. A **148**, 359 (1990).
- ⁴⁴A. R. Goñi, A. Pinczuk, J. S. Weiner, J. M. Calleja, B. S. Dennis, L. N. Pfeiffer, and K. W. West, Phys. Rev. Lett. **67**, 3298 (1991).
- ⁴⁵A. Gold and A. Ghazali, Phys. Rev. B **41**, 7626 (1990).
- ⁴⁶A. Schmeller, A. R. Goñi, A. Pinczuk, J. S. Weiner, J. M. Calleja, B. S. Dennis, L. N. Pfeiffer, and K. W. West, Phys. Rev. B **49**, 14 778 (1994).
- ⁴⁷H. Mayaffre, P. Wzietek, C. Lenoir, D. Jérôme, and P. Batail, Europhys. Lett. **28**, 205 (1994).